

49

ИНСТИТУТ ЯДЕРНОЙ ФИЗИКИ  
СО АН СССР

V.M.Aulchenko, A.D.Bukin, I.B.Vasserman,  
V.N.Getmanov, P.M.Ivanov, I.A.Koop, L.M.Kurdadze,  
S.I.Mishnev, E.V.Pakhtusova, S.I.Serednyakov,  
V.A.Sidorov, A.N.Skrinsky, G.M.Tumaikin,  
A.G.Khabakhpashev, A.G.Chilingarov, Yu.M.Chatunov,  
B.A.Shwartz, S.I.Eidelman

SEARCH FOR RESONANCES IN  $e^+e^-$  - COLLISIONS  
IN THE MASS REGION 1.0-1.4 GeV

ПРЕПРИНТ ИЯФ 79-65

Новосибирск



SEARCH FOR RESONANCES IN  $e^+e^-$  - COLLISIONS  
IN THE MASS REGION 1.0-1.4 GeV

V.M.Aulchenko, A.D.Bukin, I.B.Vasserman,  
V.N.Getmanov, P.M.Ivanov, I.A.Koop, L.M.Kurdadze,  
S.I.Mishnev, E.V.Pakhtusova, S.I.Serednyakov,  
V.A.Sidorov, A.N.Skrinsky, G.M.Tumaikin,  
A.G.Khabakhpashev, A.G.Chilingarov, Yu.M.Shatunov,  
B.A.Shwartz, S.I.Eidelman

Institute of Nuclear Physics  
630090, Novosibirsk 90, USSR

A b s t r a c t

At the storage ring VEPP-2M the scanning was performed in the energy region  $2E = 1.0 - 1.4$  GeV. No new resonances with the width up to 10 MeV have been found. For this energy region the upper limit for a lepton width  $\Gamma(\nu \rightarrow ee)$  of vector mesons with decay modes of  $\pi^+\pi^-$ ,  $K^+K^-$ ,  $\omega\pi^0$  and  $4\pi^\pm$  was obtained.

Submitted to the International Symposium on Lepton and Photon Interactions, Batavia, USA, 1979.







photomultiplier. In the further data processing the amplitudes from each scintillation counter were used <sup>for</sup> the separation of electrons and mesons.

The first shower chamber is situated after  $2 X_0$  and the second one - after  $4 X_0$  of sandwich matter. Shower chamber represents two adjoining spark gaps, <sup>with</sup> made of foiled plastic sheets electrodes. The electrodes surface is divided by narrow (1 mm) etched lines into conducting strips of 12 mm width. The spark gap is 10 mm. The read-out of information is performed from all electrodes (coordinates X and Y) with the help of ferrite core memory. The shower chambers serve mainly for the photon shower coordinates determination.

The range part of the detector involves three spark chambers located subsequently after iron blocks of 39, 47 and 63 g/cm<sup>2</sup> thickness, respectively. The construction of the range chambers is similar to that of the shower ones. Only the width of the electrode strips is 20 mm.

Time-of-flight system. Time-of-flight measurement is performed between the scintillation counters of the third layer (C3-1 and C3-2) of the opposite quadrants. The distance between counters is 60 cm (2 nsec). The resolution time of this system is  $\sigma_{t.o.f.} = 0.25$  nsec. The fast selection by the time-of-flight is performed only for the "collinear" trigger type and it permits to decrease the detector triggering rate <sup>due</sup> to the cosmic ray particles by a factor of more than 10. Besides, the value of time-of-flight is recorded with all the rest information of event on the magnetic tape.

Synchronization of the detector trigger with the time of the beam flight through the interaction region is arranged for additional decrease of the cosmic ray triggering rate. Besides, the time interval between the trigger of the time-of-flight counter of each quadrant and the moment of beam flight is measured. Later this information is used for the slow particles (kaons) selection.

The trigger of the detector can occur in several ways:

- 1) collinear events - the trigger by two charged partic-

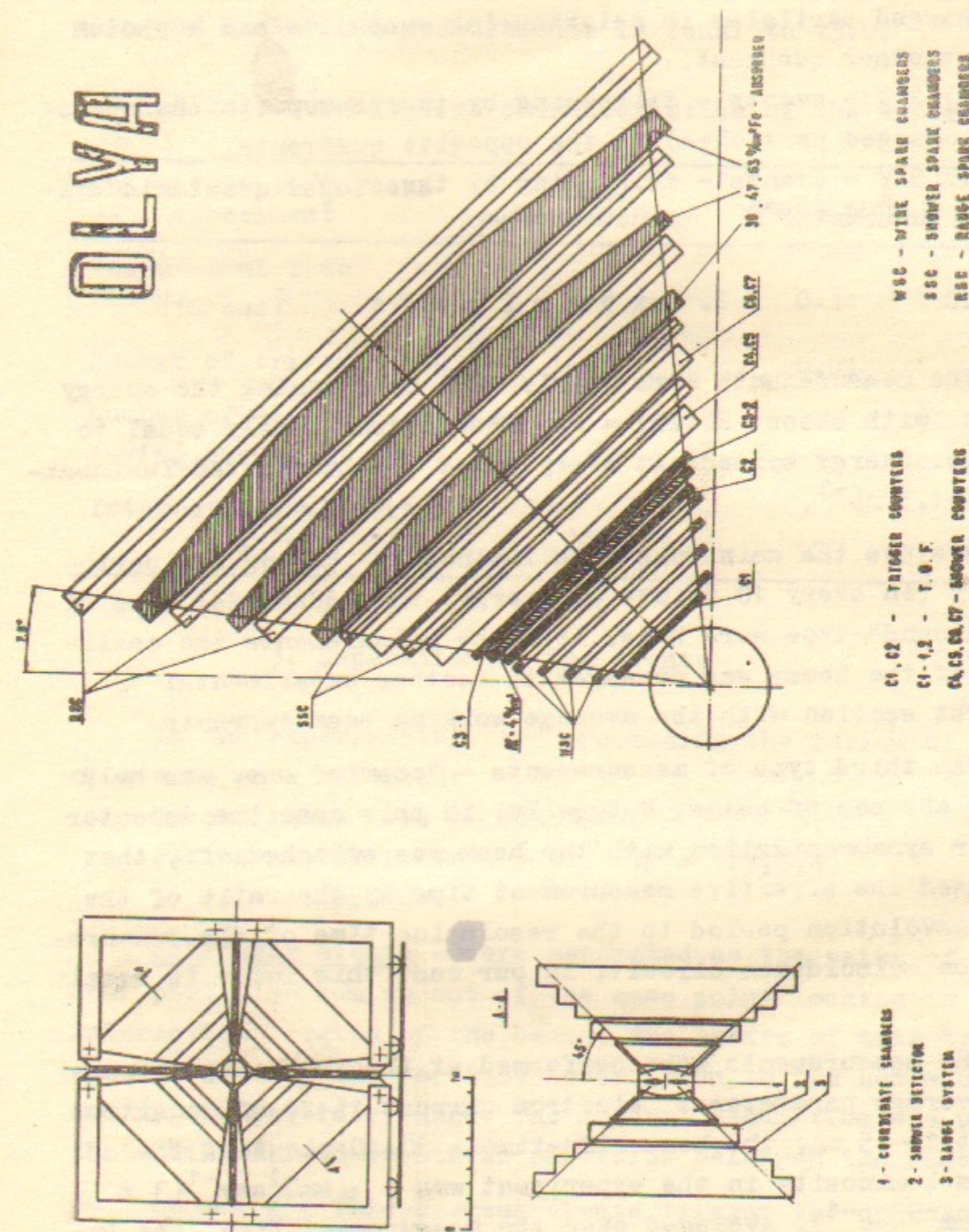


Fig.1. The lay-out of the "OLYA" detector.



les in the opposite quadrants. In both of these quadrants the three-fold coincidence of the first three scintillation counters is necessary. A triggering threshold is 45 MeV for pions and 65 MeV for kaons,

2) two noncollinear particles + photon - triggering by two charged particles in neighbouring quadrants and a photon in some other quadrant,

3) 2  $\gamma$  - events - triggering by two photons (in the absence of charged particles) in the opposite quadrants,

4) 3  $\gamma$  - events - triggering by three  $\gamma$  - quanta in different quadrants.

## 2. Experiment

The measurements were carried out by scanning the energy region with steps  $\Delta(2E) = 0.67$  MeV approximately equal to the c.m. energy spread. At every point the integrated luminosity was  $1.5 \text{ nb}^{-1}$ .

Besides the main runs with luminosity taking on, periodically (in every 10 points of energy) the additional runs of "background"-type were held. At those measurements the collisions of the beams was arranged in another experimental straight section with the average working beam currents.

The third type of measurements - "cosmic" one, was held in the absence of beams. Naturally, in this case the detector trigger synchronization with the beam was switched off, that increased the effective measurement time by the ratio of the beam revolution period to the resolution time of the synchronization coincidence circuit. In our case this ratio is equal to 10.

The measurements were performed at the following storage ring average parameters: electron current 15-20 mA, positron current 10-15 mA, the beam life-time - 30-40 minutes. The maximum luminosity in the experiment was  $3 \mu\text{bn}^{-1}\text{sec}^{-1}$  ( $3 \times 10^{30} \text{ cm}^{-2}\text{sec}^{-1}$ ). Averaged over the measurement time the luminosity was equal to  $0.7 \mu\text{bn}^{-1}\text{sec}^{-1}$  ( $0.7 \cdot 10^{30} \text{ cm}^{-2}\text{sec}^{-1}$ ). The detector triggering rate was about 1 Hz. Quantitative charac-

teristics of the experiment are presented in Table 1. The measurement time in the column "cosmic" is multiplied by a normalization factor. The background normalization has been done according to the integrated product of the circulating currents. In our experiment the ratio of this integral at the main and background measurements is equal to 13.0.

Table 1. Quantitative characteristics of the experiment

Characteristic of the experiment	Main measurements	Background	Cosmic
Measurement time [ $10^6 \text{ sec}$ ]	1.02	0.11	$0.62 \times 10.0$
Number of triggers [ $10^6$ ]	1.32	0.01	0.16
Number of elastic scattering events [ $10^3$ ]	220.	-	-
Integrated luminosity [ $\text{nb}^{-1}$ ]	725	-	-

## 3. Separation of the events

In the experimental data processing the following types of events were selected:

- 1) collinear ( $ee \rightarrow ee, \mu\mu, \pi\pi, K^+K^-$ ),
- 2) two noncollinear +  $n\gamma$ ,  $n = 1, 2, 3, 4$ ,
- 3) (3 + 4) prongs.

Collinear events - were separated as the pairs of collinear particles coming out of the same point located in the interaction region of the beams. The events of this type were separated by the particle interaction in the sandwiches and by the particle range. The natural assumption was used that both charged collinear particles belonged the same type.

$ee \rightarrow K^+K^-$ . This process events trigger the detector from the energy  $2E = 1.1$  GeV. The kaon velocity in our energy interval still noticeably differs from the unity:  $\beta(E = 0.56) = 0.47$  and  $\beta(E = 0.7) = 0.71$ . This allows to separate these



events by the pulse heights in the triggering counters (C1, C2 and C3).

For separation events were taken satisfying except the mentioned above criteria the collinearity conditions:

$$|\Delta\varphi| < 3^\circ \quad \text{and} \quad |\Delta\theta| < 5^\circ$$

In order to increase the relative part of kaons there was imposed the additional requirement that both particles would not reach the second range chamber (the range about  $130 \text{ G/cm}^2$ ).

Collinear events, satisfying these conditions, were divided into the charged kaons and the particles with the minimum ionization by the method of correlation matrix /2/. The separation parameter was the ratio of the likelihood functions for the pulse heights in the scintillation counters C1, C2 and C3 for kaons and minimum ionizing particles. More detailed description of the kaon selection procedure is done in /3/.

After the kaon extraction all the rest collinear events were divided into three classes by the range:

- 1) both particles have the total range (more than  $180 \text{ G/cm}^2$  evaluated for iron),
- 2) only one particle has the total range,
- 3) both particles don't reach the last range chamber.

The probabilities for different processes events to come to any of the mentioned above classes are shown in table 2. The probabilities were calculated by the Monte-Carlo method at the energy  $2E = 1.2 \text{ GeV}$ .

Table 2. Probabilities for events to come into the classes (1), (2), (3) in %.

Process	1	2	3
$ee \rightarrow ee$	$5 \times 10^{-4}$	0.3	$\sim 100$
$ee \rightarrow \mu\mu$	95	5	$7 \cdot 10^{-2}$
$ee \rightarrow \pi\pi$	2	25	73

The probabilities are shown here to illustrate how these processes are distributed through the three classes. From Table 2 one can see that the second and third classes contain mainly the events of  $ee \rightarrow ee$  and  $ee \rightarrow \pi\pi$ . This fact allowed us to use the correlation matrix method for events separation. As the parameters for the correlation matrix we used the ratio of the likelihood functions for the pulse height distributions in the sandwich scintillation counters for the events of  $ee$  and  $\pi\pi$ . In this approach the only quantity one needs from outside is the probability for the events  $ee \rightarrow \mu\mu$  to get to the 2 and 3 classes. This probability, first, is small and, the second, is easily calculated. Such a procedure was carried out in the pion form-factor measurement /4/ and the measurement of  $\Phi \rightarrow \pi\pi$  branching ratio /5/. The total number of events  $ee \rightarrow ee$  was found as a sum of such events in the second and third classes. Starting with the obtained numbers of  $\mu\mu$ ,  $\pi\pi$  - events in 2 and 3 classes and probability for muon to traverse all the range system (this value was found by Monte-Carlo simulation /6/) the total numbers of  $ee \rightarrow \mu\mu$  and  $ee \rightarrow \pi\pi$  events were calculated.

Non-collinear two-prong events - the events with two prongs coming from the same point of the beam region containing the  $\gamma$  - quanta in the shower chambers of the quadrants, free of charged particles. As a result of analysis it became clear that a significant admixture to the events with one  $\gamma$  - quantum was due to the radiative processes like  $ee \rightarrow ee\gamma$ . These events were rejected by the acoplanarity condition: the angle between the  $\gamma$  - quantum and the plane of two charged particles should be greater than 6 degrees.

Multi-prong events - the events with three or four charged particles tracks satisfying mentioned above geometric conditions without any  $\gamma$ -s. The extraction procedure of non-collinear and multi-prong events is described in detail in /7/.

For the search of resonances four types of events were chosen:  $\pi\pi$ ,  $KK$ , non-collinear and multi-prong events. The first type corresponds to the process  $ee \rightarrow \pi^+\pi^-$ , the se-



cond one - to the process  $ee \rightarrow K^+K^-$ , the third one - to the process  $ee \rightarrow \omega\pi^0$  and the fourth one - to the process  $ee \rightarrow 4\pi^\pm$ . Experimental distributions for three of those processes are shown in Fig. 2.

#### 4. The search for resonances.

The experiment on search for new resonances, performed at the storage ring VEPP-2M in 1975 /1/, showed that there were no new narrow resonances with a large cross section ( $\Gamma_{x \rightarrow ee} < 100$  ev) in the energy region 1.0-1.34 GeV. However about at that time one of the DESY groups discovered the resonance at the energy 1100 MeV with a width about 30 MeV in the fixed target-experiment /8/. In that experiment the value of  $\Gamma_{x \rightarrow ee}$  was not directly measured. The main decay modes of this resonance also were not measured. So it was impossible to predict the result of the colliding beams experiment. Maybe a resonance with a mass equal to 1100 MeV, does exist but is difficult to detect it in the experiment with the colliding  $e^+e^-$  - beams because of the small coupling constant with  $\gamma$  - quantum. One can also suppose that the main decay mode of this resonance is pure neutral one which is detected by the "OLYA" detector with rather low efficiency. So in the present experiment an attempt was made to find the small resonances which could be hidden by the fluctuations of background. In the vector dominance model the partial decay mode of the vector meson to electron-positron pair is proportional to the area of the resonance  $\Gamma(V \rightarrow ee) \sim \int \sigma(E) dE$ , therefore in the experiment the area of the resonance or its upper limit are looked for.

The measurements of the background and cosmic types have shown that for the collinear channels there exists an insignificant part of cosmic ray background. As for noncollinear channels the machine and cosmic background is absent, and "background" for the search of the resonance is due to the non-resonant part of the  $3\pi$  and  $4\pi$  channels.

As the "background" involving all the nonresonant channels could not be measured separately, for the search of resonances

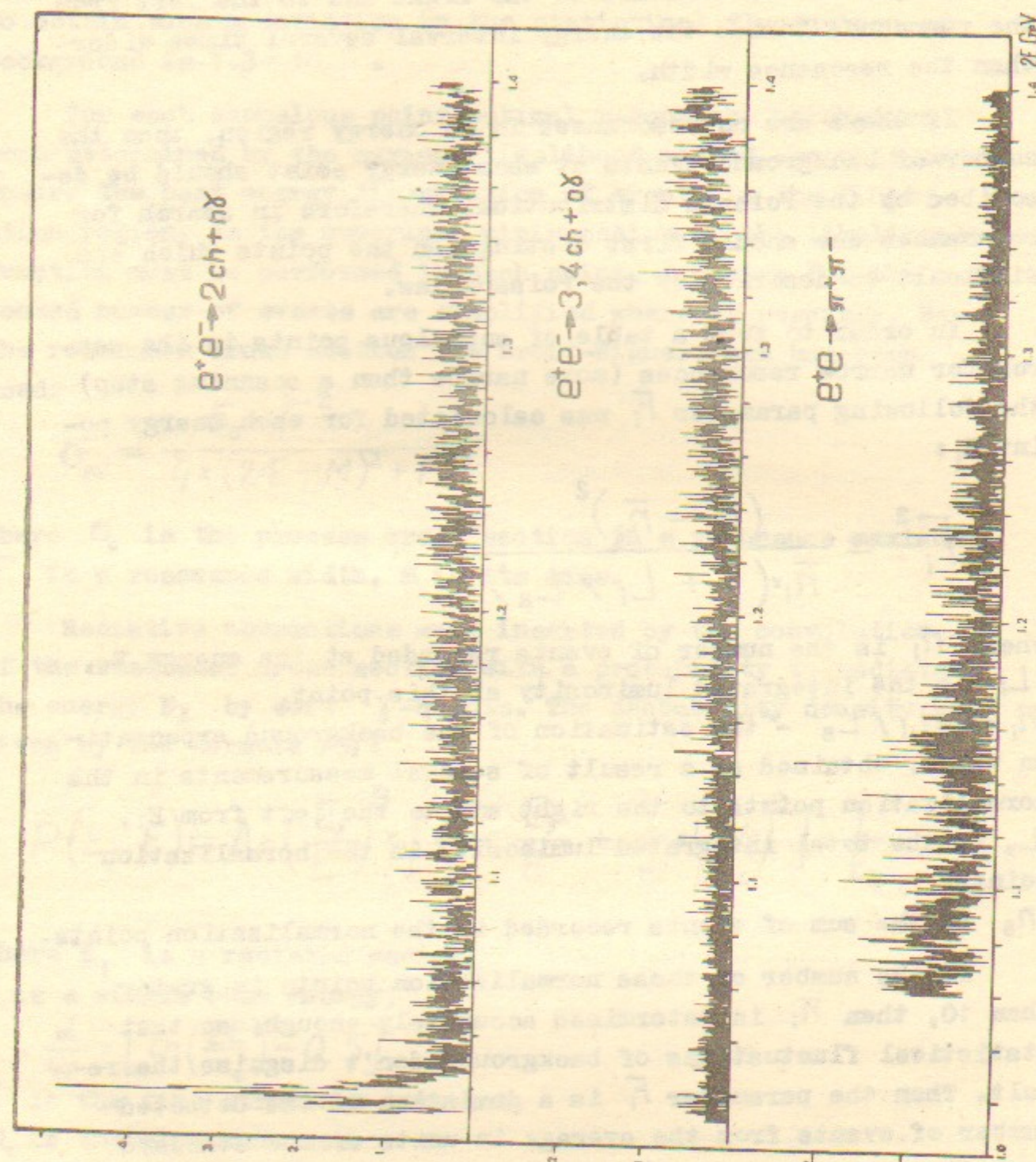


Fig. 2. Experimental cross section for the processes  $e^+e^- \rightarrow \pi^+\pi^-, \omega\pi^0, 4\pi^\pm$  (relative units).



one should accept, some assumptions concerning the background energy dependence. While the data processing we assumed that the background was constant to the right and to the left from the resonance inside the energy interval several times wider than the resonance width.

If there are no resonances in an energy region, then the number of background events at each energy point should be described by the Poisson distribution. Therefore in search for resonances one should first distinguish the points which are difficult to describe by the Poisson law.

In order to form a table of anomalous points in the search for narrow resonances (more narrow than a scanning step) the following parameter  $F_i$  was calculated for each energy point  $E_i$ :

$$F_i^2 = \frac{(n_i - \bar{n}_i)^2}{\bar{n}_i \times (1 + L_i / L_B)}$$

where  $n_i$  is the number of events recorded at the energy  $E_i$ ,  
 $L_i$  is the integrated luminosity at this point,  
 $\bar{n}_i = n_B \times L_i / L_B$  - the estimation of the background expectation value, obtained as a result of several measurements in the normalization points to the right and to the left from  $E_i$ ,  
 $L_B$  is the total integrated luminosity in the normalization points,  
 $n_B$  is the sum of events recorded in the normalization points.

If the number of these normalization points is greater than 10, then  $\bar{n}_i$  is determined accurately enough, so that statistical fluctuations of background don't disguise the result. Then the parameter  $F_i$  is a deviation of the detected number of events from the average in units of one standard deviation.

For the search for broader resonances it is sufficient to calculate the parameter  $F$  for a sum of the corresponding number of points in the vicinity of the  $i$ -th point. Naturally, the number of normalization points must be 10 times larger.

To select anomalous (in the parameter,  $F$ ) points a critical fluctuation level  $F > 3$  has been set. The probability to obtain such a deviation by the statistical fluctuation of background is  $1.3 \times 10^{-3}$ .

For each anomalous point optimal resonance parameters were determined by the maximum likelihood method, so that to ensure the best energy distribution of events in the fluctuation region. As the numerical minimization of the likelihood function must be performed in each point, formulae for the expected number of events are simplified wherever possible. For the resonance cross section the Breit-Wigner form has been used:

$$\sigma_{BV} = \frac{\sigma_0 \times \Gamma^2}{4 \times (2 \times E - M)^2 + \Gamma^2}$$

where  $\sigma_0$  is the process cross section in a resonance maximum,  $\Gamma$  is a resonance width,  $M$  is its mass.

Radiative corrections were inserted by the convolution of the resonance cross section with a probability to radiate the energy  $E_\gamma$  by soft  $\gamma$ -quanta. The probability density is given by the formula /9/:

$$P(E_\gamma, E) = A \times \left(\frac{E_\gamma}{E}\right)^B \times \left[1 - \frac{E_\gamma}{E} + \frac{1}{2} \times \left(\frac{E_\gamma}{E}\right)^2\right] \times \frac{1}{E_\gamma}$$

where  $E_\gamma$  is a radiated energy,

$E$  is a single beam energy,

$$B = \frac{\alpha}{4\pi} \times \left[\ln\left(\frac{2E}{m_e}\right) - 0.5\right],$$

$\alpha$  is the fine structure constant,

$m_e$  is the electron mass,

$$A = B \times [1 + 0.75 \times B].$$

For narrow resonances the integration region in the convolution can be increased up to infinity, not influencing the accuracy. The cross section  $\sigma_{RC}$  with radiative corrections can be expressed in this case through elementary functions (see, for example, /10/). For not very narrow resonances the



correction for the beam energy spread is small for the observed cross section and the resonance width, while for the parameter of interest - resonance area - it equals zero. Therefore this correction was included approximately as the effective broadening and lowering of the resonance curve.

In the vicinity of the chosen point the detection cross section  $\sigma(E)$  for events of some class can be written as a sum of the <sup>above</sup>resonance cross section and the non-resonant background. The expectation value  $\bar{n}_i$  for the number of events in the  $i$ -th energy point is obtained as a product of the detection cross section and the integrated luminosity collected in this point. The total logarithmical likelihood function  $\mathcal{L}$  in some interval including the explored point is written as a sum of each point contributions  $\mathcal{L}_i$ :

$$\mathcal{L}_i = \bar{n}_i - n_i + n_i \times \ln\left(\frac{n_i}{\bar{n}_i}\right)$$

Here  $n_i$  is a number of events detected in the  $i$ -th point. For each anomalous point summation covers all the points including normalization ones.

The likelihood function  $\mathcal{L}$  depends on four free parameters: resonance mass  $M$ , resonance cross section in the maximum  $\sigma_0$ , resonance width  $\Gamma$  and cross section of background detection  $\sigma_b$ . To obtain an upper limit for the resonance area the parameter  $\Pi = \sigma_0 \times \Gamma$  is convenient, which is proportional to the resonance area. Therefore  $\sigma_0$  was replaced by  $\Pi$ .

As a result of data processing optimal parameters of a possible resonance have been determined for each point with a large fluctuation. In each case one of the two following hypotheses was to be chosen: i/ experimental distribution of detected events is due to the background fluctuation, ii/ there exists a resonance in this point with parameters obtained by optimization. As a criterium to choose we used the probability to obtain such an experimental distribution due to the background fluctuation. To calculate this probability experimental points lying in the interval equal to the resonance width around its mass have been used (mass and width taken

from the optimization). For all anomalous points the probability to observe the experimental distribution due to the background fluctuation varied from  $1.6 \times 10^{-5}$  to  $1.3 \times 10^{-3}$ . Taking into account that data processing covered 500 experimental points in four independent channels the probability to obtain in the whole experiment the deviation greater than the maximum detected one was  $500 \times 4 \times 1.6 \times 10^{-5} = 0.03$ .

## 5. Results

Data processing described above gave the following results. No new resonances were observed in the energy region  $2E$  from 1060 up to 1400 Mev. The upper limits for a partial decay width  $\Gamma(V \rightarrow ee)$  have been obtained at 90% confidence level under different assumptions about the resonance width and its decay channel (Table 3).

To determine the upper limit on  $\Gamma(V \rightarrow ee)$  the corresponding detection efficiencies are needed. In Table 3 they are presented for the average energy of the interval explored. The variation at the interval ends doesn't exceed 10% of the given values. The energy range  $1000 < 2E < 1060$  Mev is more complicated for data processing because of the  $\phi$ -meson, therefore it is not included in the Table.

Table 3. Upper limits on  $\Gamma_{V \rightarrow ee} \times B_{V \rightarrow f}$  90% c.l.

Decay channel	Detection efficiency, %	Upper limit (ev)	
		1 Mev	10 Mev
$e^+e^- \rightarrow \pi^+\pi^-$	38	12	13
$e^+e^- \rightarrow K^+K^-$	36	5	9
$e^+e^- \rightarrow \omega\pi^0$	9	22	31
$e^+e^- \rightarrow 4\pi^\pm$	27	3	13

Thus in the energy region explored at 90% c.l. no narrow ( $\Gamma < 10$  Mev) resonances exist with decay modes cited above and the leptonic width greater than 31 ev ( $\sim 1/40$  of that for  $\phi$ -meson).



## References

1. V.A.Sidorov, Proceedings of the 18. International Conference on High Energy Physics, v.2, p.B13, Tbilisi, 1976.
2. A.D.Bukin et al., Preprint INP 77-92, Novosibirsk, 1977.
3. P.M.Ivanov et al., Preprint INP 79-68, Novosibirsk, 1979.
4. I.A.Koop et al., Preprint INP 79-67, Novosibirsk, 1979.
5. A.D.Bukin et al., Preprint INP 79-66, Novosibirsk, 1979.
6. A.D.Bukin and S.I.Eidelman, Preprint INP 77-101, Novosibirsk, 1977.
7. L.M.Kurdadze et al., Preprint INP 79-69, Novosibirsk, 1979.
8. S.Bartalucci et al., Nuovo Cimento 49A (1979) 207.
9. G.Parrour et al., Preprint LAL 1280, Orsay, 1975.
10. Ya.I.Azimov et al., Pisma v JETP 21 (1975) 378.

Работа поступила 8.08.79г.

Ответственный за выпуск - С.Г.ПОПОВ

Подписано к печати 15.08.79г. МН 02977

Усл. л., л. печ. л., 0,9 учетно-изд. л.

Тираж 200 экз. Бесплатно.

Заказ №65

Отпечатано на ротационной машине ИЯФ СО АН СССР